Putelat, T. (2017). A Note on Frictional Slip Patterns. In A. Colombo, M. R. Jeffrey, J. T. Lazaro, & J. M. Olm (Eds.), *Extended Abstracts Spring 2016: Nonsmooth Dynamics* (Vol. 8, pp. 153). (Research Perspectives CRM Barcelona). Birkhäuser Basel. https://doi.org/10.1007/978-3-319-55642-0_27

Peer reviewed version

Link to published version (if available):
10.1007/978-3-319-55642-0_27

A note on frictional slip patterns

T. Putelat

[†]Department of Engineering Mathematics, University of Bristol, UK.
T.Putelat@bristol.ac.uk

TP acknowledges support by the UK EPSRC programme grant "Engineering Nonlinearity" (EP/K003836/1).

Abstract: A possible origin of the frictional travelling waves usually occuring between sliding interfaces is discussed: various solutions, including propagating wavetrains, pulses and fronts, can appear under rate-and-state friction from homoclinic or heteroclinic bifurcations.

Introduction. The understanding of the spatio-temporal dynamics of frictional slip along extended solid interfaces is of great importance, both theoretically and in practice, across many industrial or natural contexts such as brake squeal or earthquake mechanics. Various regimes of stick-slip travelling waves are often observed numerically as for instance in the recent simulations of a brake pad [**2**], or experimentally as in the careful monitoring of friction rupture fronts controlling the onset of frictional slip [**6**]. The intricate nature and diversity of earthquakes recorded over the past decade ranging from aseismic events, episodic tremors, slow and fast earthquakes is also most startling, e.g. see [**11, 9**]. The emergence of such a variety of inhomogeneous frictional sliding modes, either in engineering or geophysical contexts, is a difficult problem due to its multiple scales nature caused by the complexity of the friction phenomenon, its modelling and its coupling with the elastic wave radiation. Even in the case of the idealised situation of a long thin elastic plate, a plethora of solution types, including propagating wavetrains, pulses and fronts, can appear under non-monotonic rate-and-state friction from homoclinic or heteroclinic bifurcations [**14**]. Here we briefly sketch the analysis for visco-elastic rate-and-state friction models motivated by the experimental results reported in [**7**].

Rate-and-state friction. The phenomenological rate-and-state framework of friction [**16, 1, 13**] is a physically motivated smooth regularisation of Coulomb friction where three crucial experimental observations are incorporated, namely: the time dependence of static friction in quasi-stationary contact and the velocity dependence of dynamic friction, together with sliding memory effects via an interfacial state variable $\phi(t)$ quantifying the interface resistance to slip whose characteristic relaxation timescale is denoted t_*. Accordingly classical rate-and-state models are usually defined by the pair of empirical equations

$$\tau = F(v, \phi; \sigma) \quad \text{and} \quad \dot{\phi} = -g(v, \phi; \sigma)/t_*, \tag{1}$$

where the interfacial shear stress τ depends on the interfacial slip rate v, state ϕ and normal stress σ, which is considered uniform here. A classical realisation is given by the Dieterich law defined by $F/\sigma := \mu_* + a\ln(v/V_*) + b\ln(\phi)$ and $g := \phi v/V_* - 1$ [**16**]. Such friction models are remarkably 'universal' across a wide variety of materials and can be microphysically justified from Eyring's theory of thermally activated rate processes (cf. [**12**]), which determine that the irreversible contribution to the interfacial slip rate is

Research Perspectives CRM Barcelona, Spring 2016, vol. 9, in Trends in Mathematics
Springer-Birkhuser, Basel

a nonlinear function $v_{\rm irr} = f(\tau, \phi; \sigma)$. To extend the domain of validity of this framework into the moderate to high frequency domain, experimental observations [**3, 5, 7**] suggest to take into account the elastic deformation of the contact region from the introduction of an interfacial shear stiffness k. Hence, the total interfacial slip rate v results from the sum of these elastic and irreversible contributions, i.e. $v = \dot\tau/k + f(\tau, \phi; \sigma)$, or equivalently

$$\tau = F(v - \dot\tau/k, \phi; \sigma). \tag{2}$$

Classical rate-and-state friction models are formally recovered from (2) with $k \to \infty$.

Problem formulation. Lying on a flat and rigid horizontal foundation, the sliding of a thin elastic plate of arbitrary wide extent driven by a constant shear stress $\bar\tau := \bar\mu\bar\sigma$ applied at its top and subjected to a uniform pressure $\bar\sigma$ is considered. The plate's thickness, density, Young's modulus and Poisson's ratio are respectively denoted h, ρ, E and ν. In the limit of large wavelength of the plate longitudinal wave ($\lambda \gg h$), the distribution of the longitudinal stress and displacement components can be assumed uniform across the plate's cross-section [**10**]. The equation of motion of the plate then follows from considering the balance of forces applied to a cross-section of infinitesimal width. Coupled with rate-and-state friction $(1)_2$–(2), a dimensionless 'shallow layer' approximation to the three-dimensional elasto-dynamic equations is derived as, with abuse of notation[1],

$$u_{,tt} - u_{,xx} + \tau = \bar\tau, \qquad \tau_{,t} = \kappa[u_{,t} - f(\zeta\tau, \phi)], \qquad \phi_{,t} = -rg(u_{,t}, \phi), \tag{3}$$

where $u(x,t)$ is the plate horizontal displacement. Denoting c_l the slab's longitudinal wavespeed defined by $c_l^2 = E/[\rho(1-\nu^2)]$, the key dimensionless parameters characterising the interplay between the elastic and frictional waves are $\zeta = (\rho c_l)/(\bar\sigma/V_*)$, $r = (h/c_l)/t_*$ and $\kappa = (kh)/(\rho c_l^2)$. Typically $r \ll 1$ represents the ratio of the perturbation propagation characteristic timescale over the characteristic interface rejuvenation timescale, whereas $\zeta \propto \bar\sigma^{-1} \ll 1$ is the ratio of the mechanical and interfacial impedances. Due to the large value of the interfacial stiffness ($> 10^{12}$ Pa/m), we expect $\kappa \gg 1$. We note however that such an interfacial stiffness could result from some interfacial gouge/wear instead of interfacial asperities, which could in turn reduce the order of magnitude of κ.

Within the travelling coordinate system $z := r(t + x/V)$ and denoting $v := r du/dz$, the travelling-wave reduction of (3) leads to the multiple timescale dynamical system

$$\gamma dv/dz = \tau - \bar\tau, \quad d\tau/dz = (\kappa/r)[v - f(\zeta\tau, \phi)], \quad d\phi/dz = -g(v, \phi), \tag{4}$$

whose solution types and bifurcation structure are briefly described in what follows as the key parameters $\bar\tau$ and $\gamma := r(1 - V^2)/V^2$ are varied.

Stability of uniform sliding. The study of the stability of a uniform sliding state (v_0, ϕ_0) shows that the wavelength of linear waves is consistent with the long-wave approximation and that the interfacial stiffness is stabilising. The growth rate of an infinitesimal perturbation $\delta u := (u_{,t}, \phi) - (v_0, \phi_0) = (\hat v, \hat\phi)\exp[i(\omega t - kx)]$ is governed by the dispersion relation

$$k^2 - \omega^2 - i\omega\beta(\omega) = 0 \quad \text{in which the ratio} \quad \beta(\omega) = -\frac{rg_{,\phi}F'_{ss} + i\omega F_{,v}}{(rg_{,\phi} + i\omega)(1 + i\omega F_{,v}/\kappa)}, \tag{5}$$

[1]Note that all symbols are dimensionless quantities in what follows.

represents the friction frequency response function defined and measured in [**7**]. It can be shown (see also [**15, 16**]) that uniform and steady sliding is unstable for velocity-weakening friction ($F'_{ss} < 0$), through a Hopf bifurcation with critical angular frequency ω_c, to long wavelength perturbations whose wavenumbers satisfy $k < k_c$, where $k_c^2 = \omega_c^2\big\{1 + \big[rg_{,\phi}(F_{,v} - F'_{ss})\big]/\big[(rg_{,\phi})^2 + \omega_c^2\big]\big\}$ with $\omega_c^2 = -(rg_{,\phi})^2(F'_{ss}/F_{,v})/\big[1 + rg_{,\phi}(F_{,v} - F'_{ss})/\kappa\big]$. Along with examples of friction curves, Fig. 1(A) shows an example of domain of unstable wavelengths $\lambda > \lambda_c = 2\pi/k_c$. The interfacial stiffness increases λ_c which means its effect is stabilising. Besides, as the critical wavenumber for the Dieterich law reads $\bar{k}_c^2 = (r/\zeta)(b-a)(1 + r\zeta v^2/a)$ and bounds the instability domain, we can conclude that the long-wave approximation $\lambda_c \gg 1$ remains valid provided $r/\zeta \ll 4\pi^2/(b-a)$.

Variety of solution types. Varying the shear stress $\bar{\tau}$ between the local extrema of a spinodal friction model [**13**], we find the occurrence of travelling self-healing 'slip pulses', reminiscent of the pulses described by Heaton [**8**], arising from a homoclinic bifurcation of travelling periodic slip patterns born in a Hopf bifurcation promoted by velocity-weakening friction, see Fig. 1(B,C). Such slip pulses are anchored at the equilibrium saddle point lying on the low-velocity-strengthening branch of the friction curve. Interestingly, the existence of a high velocity strengthening branch also allows the existence of 'stick pulse' which corresponds to a narrow travelling 'stick' zone. Along the bifurcated branch, travelling wave-trains of slip pulses develop from a canard explosion, which can lead either to wave-trains of slip or stick pulses. Heteroclinic connections corresponding to travelling 'detachment' (similar to [**6, 4**]) or 'attachment' fronts promoting the slab acceleration or deceleration are also possible. When the interfacial stiffness is neglected, these saddle-saddle connections exist on lines within a $(\gamma, \bar{\mu})$ phase diagram and delineate domains of generic travelling fronts and wave-trains of different types (see Fig. 1(D) and [**14**] for more details). The effect of κ on the topology of this phase diagram is under current investigation and will be published elsewhere. We note however that this bifurcation structure also strongly depends on the mathematical details of the friction model, in particular the state evolution equation. For instance the classic monotonic Dieterich-Ruina friction models [**16**] only allows for wave trains of slip-pulse solutions in an exponentially narrow window of $\bar{\tau}$.

Conclusion. This work shows how introducing a smooth and non-monotonic rate-and-state interfacial friction model allows for the existence of different localised modes of frictional slippage as saddle-saddle connections with slip or stick pulses, detachment or attachment fronts along with travelling wavetrains, all in the same mathematical formulation of regional contact and within the well established theory of smooth dynamical system and global bifurcations. Careful consideration of the choice of the non-monotonic friction law and the type of interfacial state kinetics is necessary to capture the full richness of wave types. In such an idealised configuration of a thin elastic slab, this plethora of behaviours and the question of their physical selection may explain why friction experiments are difficult and associated with challenging repeatability issues [**17**]. This work may also shed new light on the complex and diverse dynamics of earthquake ruptures in particular with respect to the large variability of earthquake duration and frequency spectrum [**11, 9**]. Future work will explore the possibility of complex or irregular patterning from Shilnikov bifurcation or bursting dynamics scenarii that the three dimensional phase space and the slow-fast multiscale nature of system (4) may allow.

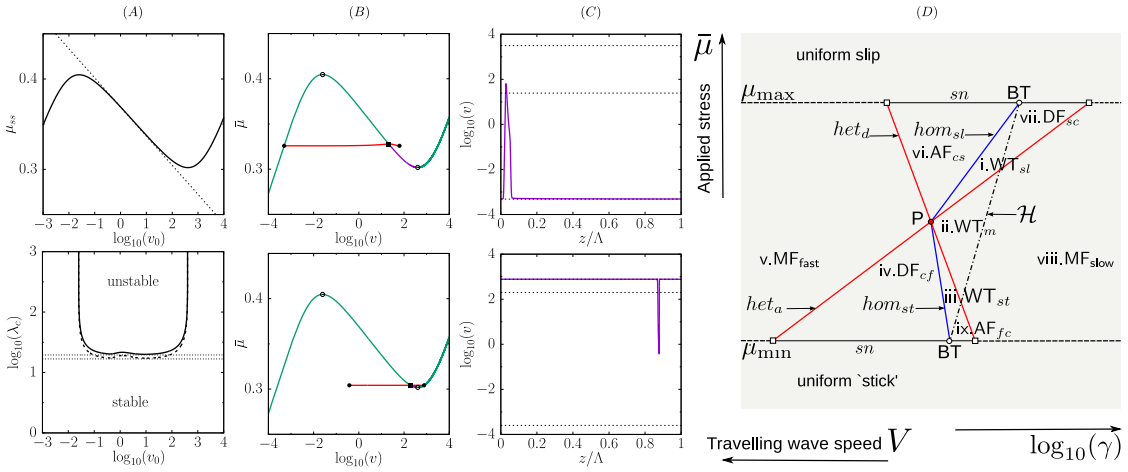

FIGURE 1. (A) Steady-state friction characteristics and corresponding critical wavelengths λ_c ($r = 10^{-6}$, $\zeta = 10^{-7}$): $\kappa = 1$ (solid line), $\kappa \to \infty$ (dashed line). The domain of unstable wavelengths is limited to the domain of friction velocity weakening (dotted lines: monotonic friction). (B) Typical bifurcation diagrams for (4) under spinodal friction [**13**] leading to homoclinic connections (•) from the growth of wavetrains born at a Hopf bifurcation (■) (the red lines correspond to the maximum and minimum amplitude along the branch of periodic orbits): (top) slip pulse, (bottom) stick pulse. (C) Numerical approximations of slip pulse (top, $\gamma = 10^{-4}/\zeta$) and stick pulse (bottom, $\gamma = 10^{-6}/\zeta$) of period $\Lambda = 100$ for $\kappa = 100(r/\zeta)$ (the dotted lines delineate the three uniform sliding states). (D) Sketch of typical phase diagram of travelling wave patterns ($\kappa \to \infty$, see [**14**]): loci of slip pulses (hom_{sl}), stick pulses (hom_{st}), detachment fronts (het_d), attachment fronts (het_a) as saddle-saddle connections; Hopf bifurcation locus ($\mathcal{H}$); saddle-node bifurcation loci at the local extrema of friction (sn); Stick-slip wave-trains (WT). Generic detachment (DF), attachment (AF) and mixed (MF) fronts as saddle connections to the equilibrium point of the velocity weakening branch. Takens-Bogdanov points (BT). Uniform slab's slip rates solve $\mu_{ss}(v) \equiv \mu(v, \phi_{ss}(v)) = \bar{\mu}$ and $g(v, \phi_{ss}(v)) = 0$.

References

[1] Baumberger T. & Caroli C., Adv. Phys., **55**:279–348, (2006).
[2] Behrendt J. et al., J. Sound Vib., **330**:636–651, (2011).
[3] Berthoud P. & Baumberger T., Proc. Roy. Soc. A., **454**:1615–1634 (1998).
[4] Bouchbinder E. et al., Phys. Rev. Lett., **107**:235501, (2011).
[5] Bureau L. et al., Phys. Rev. E, **62**:6810–6820, (2000).
[6] Ben-David O. et al., Science, **330**:211–214 (2010).
[7] Cabboi A. et al., J. Mech. Phys. Solids, **92**:210–236, (2016).
[8] Heaton T.H., Phys. Earth Planet Int., **64**:1–20, (1990).
[9] Ide S., Proc Jpn Acad Ser B Phys Biol Sci. **90**:259–277, (2014).
[10] Kolsky H.: *Stress Waves in Solids.* Oxford Clarendon Press, (1953).
[11] Peng Z. & Gomberg J., Nature Geosci., **3**:599–607, (2010).
[12] Putelat T. et al., J. Mech. Phys. Solids, **59**:1062–1075, (2011).
[13] Putelat T. & Dawes J.H.P., J. Mech. Phys. Solids, **78**:70–93, (2015).
[14] Putelat T. et al. *Phase plane analysis of localised frictional waves.* Sub-judice.
[15] Rice, J.R. & Ruina A.L., J. App. Mech.,**50**:343–349, (1983).
[16] Ruina A.L., J. Geophys. Res., **88**:10,359–10,370, (1983).
[17] Woodhouse J. et al., Phil. Trans. R. Soc. A., **373**: (2015).